Journal of the Korean Society of Surveying, Geodesy, Photogrammetry and Cartography
Vol. 34, No. 2, 133-142, 2016
http://dx.doi.org/10.7848/ksgpc.2016.34.2.133
ISSN 1598-4850(Print)
ISSN 2288-260X(Online)
Original article

A Test Result on the Positional Accuracy of Kompsat-3A Beta Test Images

Oh, Jae Hong[1)]· Seo, Doo Chun[2)] · Lee, Chang No[3)]

Abstract

KOMPSAT-3A (KOrea Multi-Purpose SATellite-3A) was launched in March 25 2015 with specification of 0.5 meters resolution panchromatic and four 2.2 meters resolution multi spectral sensors in 12km swath width at nadir. To better understand KOMPSAT-3A positional accuracy, this paper reports a test result on the accuracy of recently released KOMPSAT-3A beta test images. A number of ground points were acquired from 1:1,000 digital topographic maps over the target area for the accuracy validation. First, the original RPCs (Rational Polynomial Coefficients) were validated without any GCPs (Ground Control Points). Then we continued the test by modeling the errors in the image space using shift-only, shift and drift, and the affine model. Ground restitution accuracy was also analyzed even though the across track image pairs do not have optimal convergence angle. The experimental results showed that the shift and drift-based RPCs correction was optimal showing comparable accuracy of less than 1.5 pixels with less GCPs compared to the affine model.

Keywords : Kompsat-3A, Positional Accuracy, RPCs, High-resolution Satellite Images, GCPs

1. Introduction

Kompsat-3A is a high-resolution earth observing satellite launched in Mar 25, 2015 after developed by KARI (Korea Aerospace Research Institute). Kompsat-3A satellite contains AEISS-A camera which is similar to Kompsat-3's AEISS sensor. Kompsat-3A and its AEISS-A were designed to acquire 0.55m resolution of panchromatic data as well as 2.2m resolution of multispectral data. Moreover, it can obtain 5.5m resolution of thermal image data. Table 1 shows the specification of Kompsat-3A satellite and AEISS-A sensor.

Following the launch, the geometric and radiometric calibration have been carried out by KARI (Seo *et al*., 2015). KARI conducted the locational accuracy validation based on total 94 test sites data and they reported 8.9m and 9.8m RMSE (Root Mean Square Error) for strip and one-pass stereo acquisition modes, respectively. They also reported 0.89 pixels of errors when test images were orthorectified with GPS-surveyed GCPs (Ground Control Points) and LiDAR DEM (Digital Elevation Model). After completion of the calibration/validation processes, KARI distributed beta test data for the first time in this year. The beta test data are across-track stereos acquired in different dates for the same area.

It is important for users to validate the positional accuracy of high-resolution satellite images to better understand and

Received 2016. 03. 29, Revised 2016. 04. 27, Accepted 2016. 04. 28
1) Member, Dept. of Civil Engineering, Chonnam National University (E-mail: ojh@jnu.ac.kr)
2) Satellite Information Center, Korea Aerospace Research Institute (E-mail: dcivil@kari.re.kr)
3) Corresponding Author, Member, Dept. of Civil Engineering, Seoul National University of Science and Technology (E-mail: changno@seoultech.ac.kr)

Table 1. Specification of Kompsat-3A satellite

	PAN	MS	TIR
Spectral bands	450-900 µm	Blue: 450-520 µm Green: 520-600 µm Red: 630-690 µm NIR: 760-900 µm	3.3 - 5.2 µm
GSD (Ground Sample Distance)	0.55m at nadir	2.2m at nadir	5.5 m at nadir
Focal length	8.56 m	8.56 m	1.97 m
Swath width at nadir	12 km	12 km	12 km
Data quantization	14 bit	14 bit	14 bit
CCD detector	Array of 24,000 pixels consisting of 2 stacks of 12,000 pixels each	Arrays of 4(RGB and IR) x 6,000 pixels of consisting of 2 stacks of 3,000 pixels each	Array of 2,400 pixels

use the data for precise mapping (Fraser and Ravanbakhsh, 2011; Oh *et al*., 2011; Aguilar *et al*., 2012). Therefore, in this paper, we investigated the positional accuracy of Kompsat-3A data using GCPs derived from 1:1,000 topographic maps. First, the positional accuracy of the original RPCs (Rational Polynomial Coefficients) was assessed, followed by the modeling of the errors of the RPCs using the GCPs. Several cases of parameterization were tested for the modeling such as shift-only, shift and drift, and the affine with geometric error pattern analysis. In addition, ground restitution accuracy was tested even though the across track image pairs do not have optimal convergence angle.

The paper is structured as follows: In section 2, a brief RPCs and its error modeling equations are explained. In section 3 the experimental results are presented with beta test Kompsat-3A image with GCPs, followed by conclusions in section 4.

2. RPCs and Error Modeling

RPCs refer to the coefficients of RFM (Rational Function Model). RFM is a popular replacement sensor model which is in a non-linear form of 80 unknowns (or 78 unknowns) to compute an image coordinate from a given ground coordinate (latitude and longitude) as shown Eq. (1). This model does not require information about the camera and ephemeris to perform georeferencing while it shows practically little difference in the georeferencing accuracy compared to a rigorous sensor model for a given elevation range (Grodecki, 2001).

$$Y = \frac{a^T u}{b^T u}, X = \frac{c^T u}{d^T u} \quad (1)$$

with

$$u = [1 \;\; V \;\; U \;\; W \;\; VU \;\; VW \;\; UW \;\; V^2 \;\; U^2 \;\; W^2 \;\; UVW \;\; V^3 \;\; VU^2 \;\; VW^2 \;\; V^2U \;\; U^3 \;\; UW^2 \;\; V^2W \;\; U^2W \;\; W^3]^T$$

$$U = \frac{\phi - \phi_0}{\phi_S}, V = \frac{\lambda - \lambda_0}{\lambda_S}, W = \frac{h - h_0}{h_S}, Y = \frac{l - L_0}{L_S}, X = \frac{s - S_0}{S_S}$$

$$a = [a_1 \; a_2 \cdots a_{20}]^T, b = [b_1 \; b_2 \cdots b_{20}]^T, c = [c_1 \; c_2 \cdots c_{20}]^T,$$

$$d = [d_1 \; d_2 \cdots d_{20}]^T$$

where *X*, *Y* : the normalized image coordinates, *U*, *V*, *W* : the normalized ground point coordinates, ϕ, λ, h : the geodetic latitude, longitude and ellipsoidal height of ground point, *l*, *s* : the image line (row) and sample (column) coordinates, $\phi_0, \lambda_0, h_0, S_0, L_0$: the offset factors for the latitude, longitude, height, sample and line, $\phi_S, \lambda_S, h_S, S_S, L_S$: the scale factors for the latitude, longitude, height, sample and line.

KOMPSAT-3A provides RPCs but the positional accuracy is sometimes not enough for some applications such as a large scale mapping. In that case, the accuracy of RPCs should be improved with available GCPs. This is quite simple compared to the case of the rigorous sensor modeling because the process models the geometric errors in the two-dimensional image space (Fraser and Hanley, 2005). Note that the rigorous modeling estimates the bias and drift of the satellite's position and attitude information in the three-dimensional object space. Eq. (2) is the affine-based RPCs correction model. In the model, A_0, B_0 are shift correction parameters (e.g., bias errors in satellite position or attitude), A_1, B_1 are for the drift (e.g., linear errors in satellite attitude) with line number increasing, A_2, B_2 model the remaining systematic errors (Fraser and Hanley, 2005). The estimation of these correction parameters requires good GCPs information. To this end outlier detection and removal processes are sometimes required when the reliability of GCPs is not high enough.

$$\begin{aligned} l' &= l + A_0 + A_1 l + A_2 s \\ s' &= s + B_0 + B_1 l + B_2 s \end{aligned} \tag{2}$$

where $A_0, A_1, A_2, B_0, B_1, B_2$: coefficients of the affine model for shift, drift and systematic errors, l, s : the computed image coordinates of a point (sample and line) (see Eq.(1)), l', s' : the correct coordinates of the point.

3. Experiment

3.1 Test data

The Kompsat-3A images used for the accuracy validation were acquired over Daejeon city area in Dec 22 and 29, 2015. Table 2 presents the specification of the tested Kompsat-3A. The ground sampling distance was about 60cm~76cm, which are a little larger compared to the satellite's specification due to the low elevation angles. The images are used for stereo generation but the across-track stereo quality is relatively low because the convergence angle is large such as 55.97 degrees.

Using the piecewise approach (Oh *et al*., 2010) two images were epipolar image resampled for anaglyph view as shown in Fig. 1. The piecewise approach is a epipolar resampling method developed for pushbroom sensors and it consists of two main steps; the epipolar curve point generation over the entire scene, and the establishment of epipolar image transformation.

Table 2. Specification of the Kompsat-3A data

Kompsat-3A beta test data	K3A-1	K3A-2
Acquisition date	2015-12-22, 04:25(UTC)	2015-12-29, 04:44(UTC)
Elevation/ Azimuth	61.19°/78.87°	52.97°/197.67°
Original Ground Sampling Distance (line/sample)	0.593/0.678 m	0.761/0.663 m
Image size (line/sample)	21,720×24,060 pixels	17,080×24,060 pixels
Convergence Angle	55.97°	

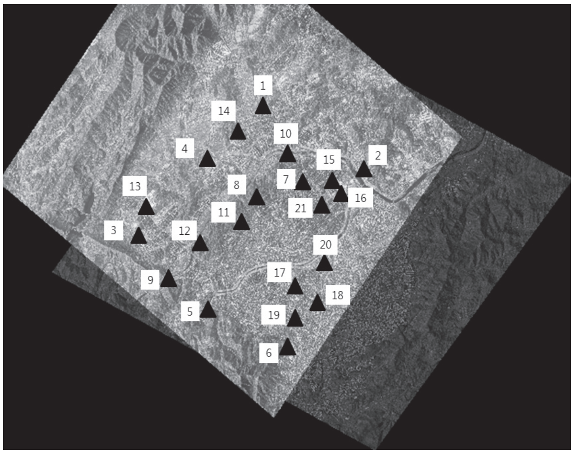

Fig. 1. Anaglyph of tested Kompsat-3A images with GCPs distribution

Total 21 GCPs (Ground Control Points) were extracted from 1:1,000 scale digital topographic maps for the accuracy validation and they are also plotted in Fig. 1. Position accuracy of the digital map is about 0.5m (1 sigma) for both of plane and height. The orthometric height was converted to the ellipsoidal height using KNGeoid14 model (Lee and Kwon, 2015). The geoid height of the study area is ranged from 25.12~25.54m.

3.2 Accuracy without any GCP

First we tested the positional accuracy of the RPCs without further adjustment. 21 GCPs were used as check points for

Table 3. Positional accuracy of RPCs [No GCP]

	K3A-1 (pixels) (sample/line)		K3A-2 (pixels) (sample/line)		Ground (m) (Lon/Lat/height)		
Mean	-19.73	-23.34	-10.16	-1.17	11.60	-6.21	1.43
RMSE	20.39	24.60	10.26	1.79	11.64	7.66	4.39
	31.95		10.42		13.93		4.39

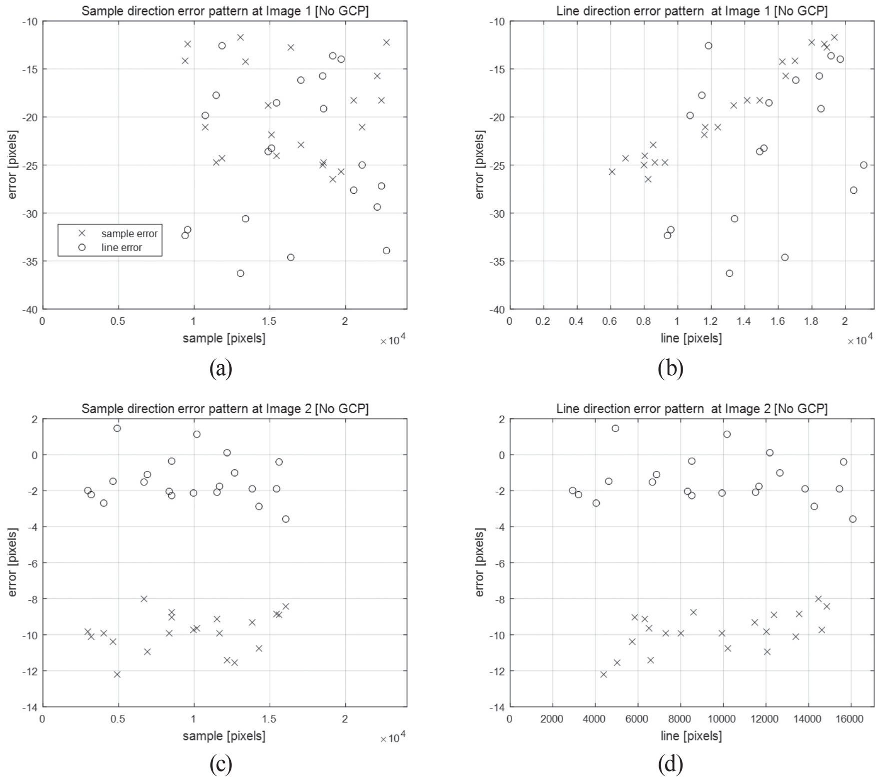

Fig. 2. Error patterns along the sample and line directions

the accuracy validation. As shown in Table 3, K3A-1 image showed 20~25 pixels of errors but K3A-2 was better in accuracy especially in y-direction. The ground restitution accuracy was 7~12 meters in horizontal direction and 4.4 meters in elevation.

Fig. 2 are the error pattern plots along the sample and line directions. In Fig. 2(a) and (b), We can clearly see larger line errors compared to sample errors of K3A-1. In Fig. 2(b) a very strong linear pattern of sample errors along the line direction is observed. In contrast, the sample and line errors in K3A-2 image in Fig. 2(c) and (d) seems quite stable without up and down though a very slight linearity is observed. We doubt the satellite was more stable when acquiring K2A-2 data.

3.3 Single GCP-based RPCs adjustment

For this experiment, single GCP was used for the RPCs correction such as a simple translation. The other 20 GCPs were used as check points for the accuracy and consistency as listed in Table 4. The errors of K3A-1 data are quite larger more than 5 pixels such that the single GCP-based correction is not optimal. The errors are greater particularly along the line direction. Moreover, the error range is wide from 5 to

Table 4. Positional accuracy of RPCs [Single GCP for RPCs shift]

Point used for shift correction	Accuracy at 20 check points in RMSE						
	K3A-1 (pixels) (sample/line)		K3A-2 (pixels) (sample/line)		Ground (m) (Lon/Lat/height)		
1	6.85	13.68	2.63	3.19	1.51	7.91	5.15
2	7.88	12.50	2.05	1.34	1.82	7.24	6.27
3	8.77	10.79	1.08	1.47	1.40	6.66	7.17
4	5.22	8.61	1.05	1.77	0.97	4.84	4.74
5	8.48	13.06	1.04	1.42	1.24	7.63	7.49
6	8.96	12.45	1.73	2.45	1.92	7.65	6.53
7	6.01	10.87	1.05	2.91	0.98	6.40	5.13
8	5.47	7.58	1.48	1.67	0.96	4.54	4.47
9	9.36	14.41	2.07	1.27	2.09	8.32	7.63
10	6.67	9.29	1.29	1.51	1.01	5.43	6.19
11	5.07	7.55	1.05	1.40	0.98	4.44	4.17
12	7.38	10.02	1.52	1.32	1.00	5.93	6.87
13	7.40	11.26	1.04	1.37	1.13	6.60	6.48
14	7.19	9.76	1.20	1.27	1.47	5.82	5.82
15	7.35	11.16	1.24	1.42	1.00	6.40	7.08
16	8.53	12.81	1.93	2.02	1.87	7.66	6.44
17	5.19	8.37	1.14	1.35	0.98	4.86	4.34
18	5.19	8.20	1.39	1.65	1.12	4.69	4.40
19	6.36	9.29	1.41	1.35	1.40	5.51	5.02
20	5.22	7.61	1.40	1.89	1.48	4.46	4.19
21	7.14	8.95	1.05	1.30	1.39	5.40	5.82

15 pixels meaning that single GCP-based corrections did not produce consistent results. In contrast, K3A-2 data shows more consistent and higher accuracy ranging about 1~3 pixels. The ground restitution accuracy was decent along the longitude direction but much worse along the latitude direction due to the large errors in K3A-1 along the line direction.

Fig. 3 plots the accuracy in each image. In the plot, bars show the mean accuracy of the other GCPs locations when the GCP was used for a RPCs correction. The mean value close to zero is preferred but K3A-1 image shows a large variation especially along the y-direction up to more than 10 pixels. In other words, the single GCP-based RPCs correction did not yield consistent accuracy. In contrast, K3A-2 image showed relatively consistent accuracy.

Fig. 4 shows the error vectors in the image space. For example, the error vector at GCP 1 indicates the mean error of the other 20 check points when GCP 1 was used for the shift correction. In K3A-1 plot, the large and different error patterns are observed between the upper and lower parts of GCPs. K3A-2 showed relatively good quality of adjustment with small and irregular error vectors.

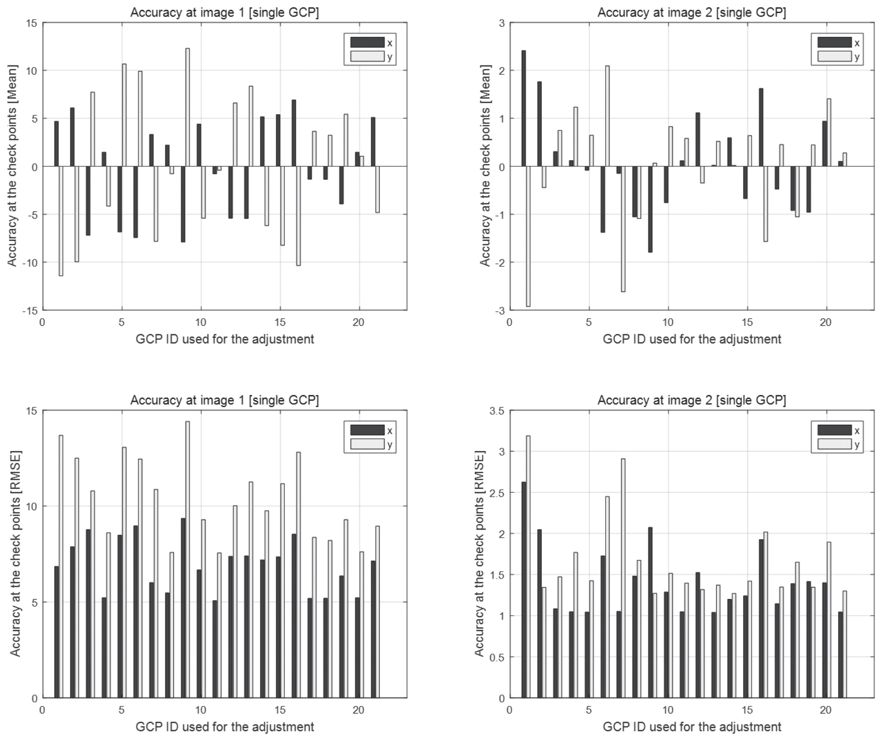

Fig. 3. Accuracy in mean and RMSE in the case of single GCP-based RPCs correction

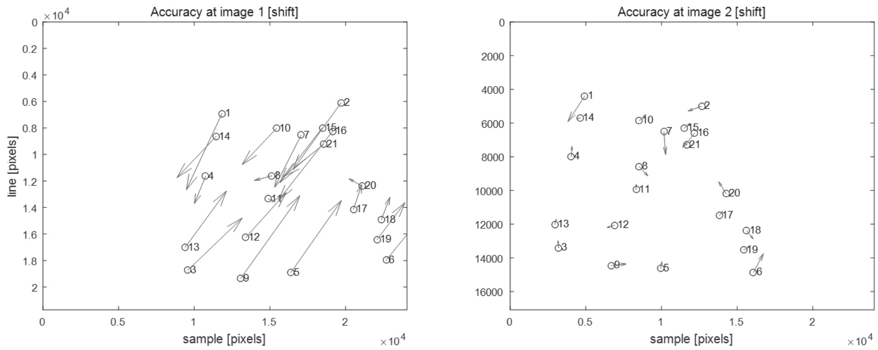

Fig. 4. The error vectors when a shift correction has been made (arrow scale: 500)

3.4 Multiple GCPs-based RPCs adjustment

Among 21 control points, we selected 8 points for GCPs and used the other points for the accuracy check. The selection of GCPs was made considering the distribution in the image space as plotted using triangles in Fig. 5. First we tried the shift and drift adjustment of RPCs. Table 5 shows the residual at GCPs and accuracy at the check points, respectively. 0.83~1.39 pixels of residuals were derived and 1.07~1.49 pixels of errors were computed. Slightly larger residuals and errors were derived along the line direction, particularly in K3A-1. In the case of the ground restitution, horizontal residuals and errors ranged from 0.50 to 0.86m

Table 5. Positional accuracy of RPCs [Multiple GCPs]

Correction model	K3A-1 (pixels) (sample/line)		K3A-2 (pixels) (sample/line)		Ground (m) (Lon/Lat/height)		
Shift and drift [residual at GCPs]	0.90	1.39	0.83	1.05	0.50	0.63	1.03
Shift and drift [errors at check points]	1.33	1.49	1.07	1.11	0.57	0.86	1.16
Affine [residual at GCPs]	0.81	1.29	0.82	1.04	0.42	0.60	1.03
Affine [errors at check points]	1.27	1.50	1.09	1.12	0.59	0.87	1.15

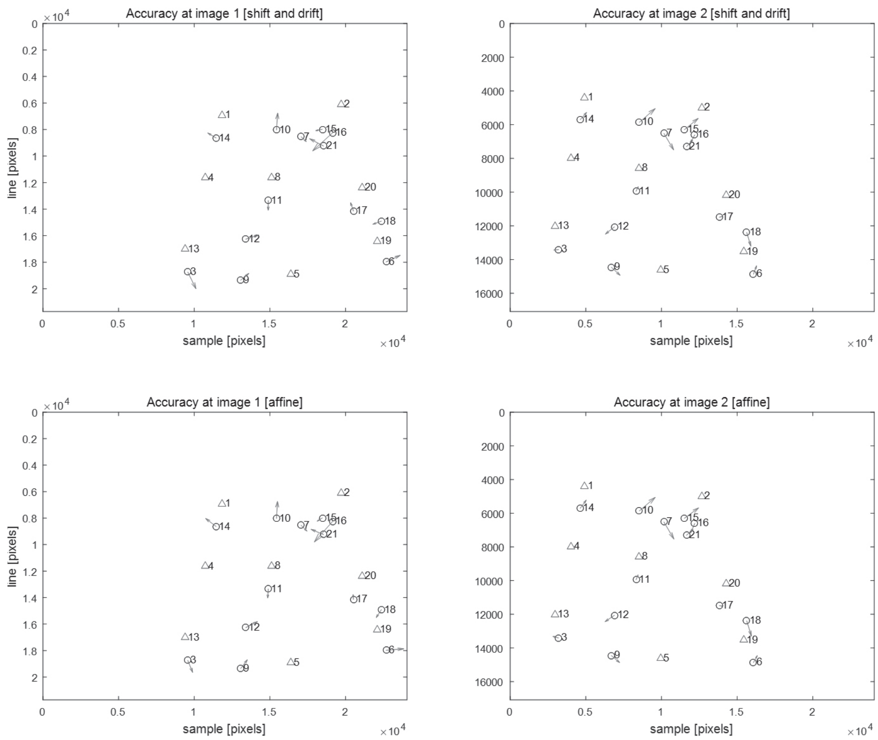

Fig. 5. The error vectors when a shift/drift and affine correction has been made with multiple GCPs (arrow scale: 500)

and the elevation residual and error are slightly higher than one meter. The result shows that using the shift and drift model could significantly reduce the large line direction errors appeared in K3A-1 data.

Next, we applied the affine-based RPCs correction using the same GCPs. As shown in Table 5, the affine-based model showed no further accuracy improvement compared to the shift and drift model. This means that most errors come from the bias and linear errors in the attitude position and attitude of Kompsat-3A. Fig. 5 present the error vector plots for the aforementioned modeling cases. The error vectors of two models showed little difference.

Table 6. Positional accuracy of RPCs [3 GCPs]

Correction model	K3A-1 (pixels) (sample/line)		K3A-2 (pixels) (sample/line)		Ground (m) (Lon/Lat/height)		
Shift and drift [Non linear distribution]	1.23	1.80	1.58	1.45	0.65	0.90	1.58
Shift and drift [Linear distribution]	1.55	2.04	1.32	1.41	0.56	1.00	1.45
Affine [Non linear distribution]	1.45	1.99	1.56	1.78	0.95	1.04	1.55
Affine [Linear distribution]	5.55	8.65	6.63	11.33	2.33	2.98	13.26

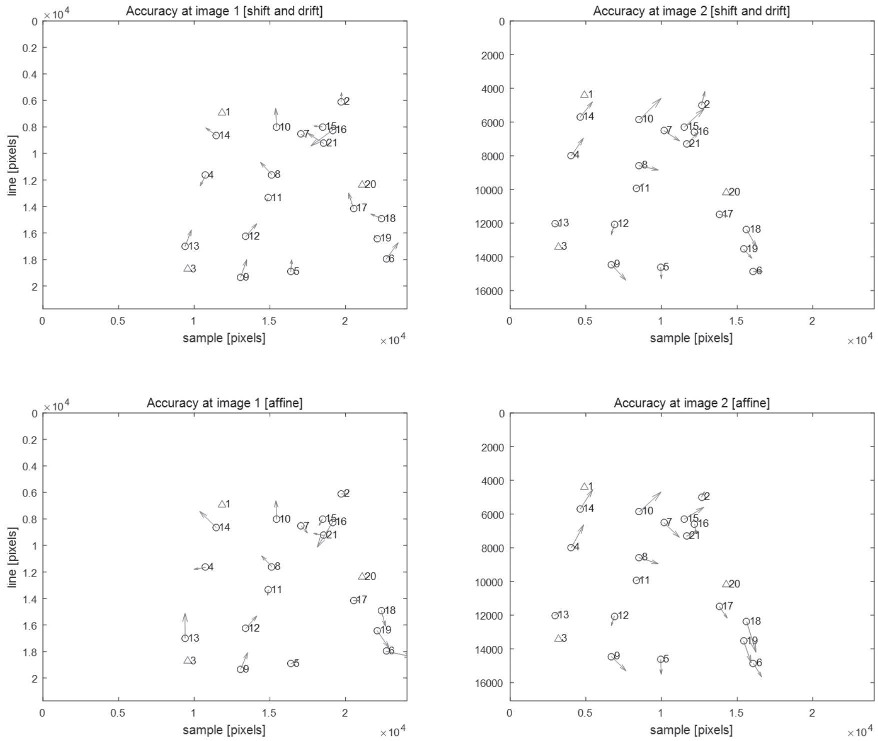

Fig. 6. The error vectors when a shift/drift and affine correction have been made with 3 non linearly distributed GCPs (arrow scale: 500)

Finally, we used just three GCPs to validate the models. In this case, we separated experiments into two sub-cases according to GCPs distributions. One sub-case is that three GCPs are distributed in a triangle shape over the region as shown in Fig. 6, and the other case is that three GCPs are linearly positioned in Fig. 7. The positional accuracy in Table 6 shows that the shift and drift model is slightly better than the affine model for the case of non-linearly distributed GCPs. However for linear GCPs distribution, the affine model showed very poor results that can be easily predicted.

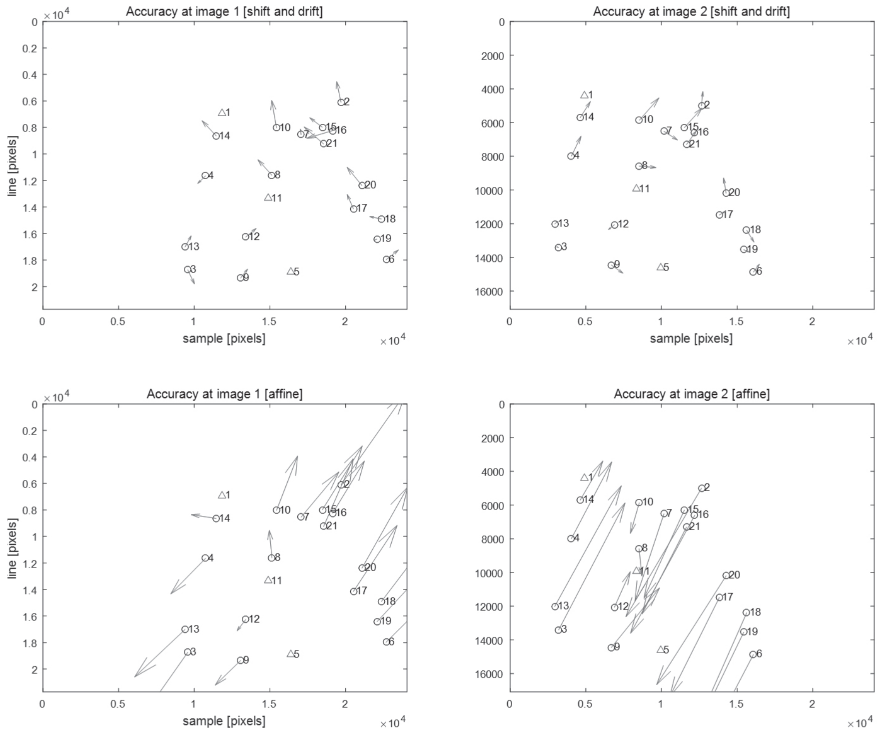

Fig. 7. The error vectors when a shift/drift and affine correction have been made with 3 linearly distributed GCPs (arrow scale: 500)

In contrast, the shift and drift model could secure one meter level of horizontal mapping accuracy with linearly distributed GCPs. Fig. 6 and Fig. 7 present the error vector plots for the two cases.

4. Conclusion

Kompsat-3A is a high-resolution earth observing satellite launched in Mar 25, 2015. KARI released first beta test images and we investigated the positional accuracy of the data. We studied the accuracy for several cases including no GCP, single GCP, and multiple GCPs for parameterization of RPCs. Test results could be summarized as below.

1. The original RPCs of Kompsat-3A beta test across-track stereo data showed 10~32 pixels of errors in the image space, and 13.9 meters of horizontal errors and 4.4 meters of elevation errors in the object space.
2. One of the beta test images showed very strong linear pattern of sample errors and this pattern prevents successful single GCP-based RPCs correction.
3. The linear pattern along the line direction was successfully corrected using a shift and drift model.
4. The shift and drift model produced little difference compared to the affine model showing less than 1.5 pixels of image errors with sub-meter levels of horizontal accuracy in the object space.
5. With just three GCPs, the shift and drift model produced better result compared to the affine model, particularly when the GCPs distribution is poor.

For the future study, we plan to investigate the effect of the image acquisition geometry to the positional accuracy.

Acknowledgment

This study was (partially) supported by Seoul National University of Science and Technology.

References

Aguilar, M.A., Aguilar, F.J., Saldana, M.M., and Fernandez, I. (2012), Geopositioning accuracy assessment of GeoEye-1 panchromatic and multispectral imagery, *Photogrammetric Engineering & Remote Sensing*, Vol. 78, No. 3, pp. 247-257.

Fraser, C.S. and Hanley, H.B. (2005), Bias-compensated RPCs for sensor orientation of high-resolution satellite imagery, *Photogrammetric Engineering & Remote Sensing*, Vol. 71, No. 8, pp. 909-915.

Fraser, C.S. and Ravanbakhsh, M. (2011), Precise georefrencing of long strips of ALOS imagery, *Photogrammetric Engineering & Remote Sensing*, Vol. 77, No. 1, pp. 87-100.

Grodecki, J. (2001), IKONOS stereo feature extraction – RPC approach, *Proceedings of ASPRS 2001 Annual Convention*, ASPRS, 25–27 April, St. Louis, Missouri, unpaginated CD-ROM.

Lee, J.S. and Kwon, J.H. (2015), Construction and precision verification of Korean national geoid model KNGoid14, *Conference of Korean Society of Surveying, Geodesy, Photogrammetry, and Cartography*, 23-24 April, Changwon, Korea, pp. 177-179. (in Korean with English abstract)

Oh, J.H., Lee, C.N., and Seo, D.C. (2011), A test result on positional accuracy of Kompsat-2 pan imagery, *Proceedings of ASPRS 2011 Annual Conference*, 1-5 May, Milwaukee, Wisconsin, pp. 378-386.

Oh, J.H., Lee, W.H., Toth, C.K., Grejner-Brzezinska, D.A., and Lee, C.H. (2010), A piecewise approach to epipolar resampling of pushbroom satellite images based on RPC, *Photogrammetric Engineering & Remote Sensing*, Vol. 76, No. 12, pp. 1353-1363.

Seo, D.C., Hong, G.B., and Jin, C.G. (2015), Kompsat-3A direct georeferencing mode and geometric calibration/validation, *Proceedings of the 36th Asian Conference on Remote Sensing*, 19-23 Oct, Quezon City, Metro Manila, Philippines, http://a-a-r-s.org/acrs/administrator/components/com_jresearch/files/publications/TUP1-48.pdf (last date accessed: 23 March 2016).